MARMARA UNIVERSITY

FACULTY OF ENGINEERING

Design and Synthesis of Flame-Retardant PS Electrospun Nanofibers

UMUT ASLAN, UFUK FURKAN ASARKAYA

GRADUATION PROJECT REPORT

Department of Mechanical Engineering

Supervisor

Dr. Aybala USTA YILDIRIM

ISTANBUL, 2023

MARMARA UNIVERSITY

FACULTY OF ENGINEERING

Design and Synthesis of Flame-Retardant PS Electrospun Nanofibers

by

Umut ASLAN, Ufuk Furkan ASARKAYA

July 3, 2023, Istanbul

SUBMITTED TO THE DEPARTMENT OF MECHANICAL ENGINEERING IN PARTIAL FULFILLMENT OF THE REQUIREMENTS FOR THE DEGREE

OF BACHELOR OF SCIENCE

AT

MARMARA UNIVERSITY

Signature of Author(s)

.....

Department of Mechanical Engineering

Certified By

.....

Project Supervisor, Department of Mechanical Engineering

Accepted By

.....

Head of the Department of Mechanical Engineering

CONTENTS

ABSTRACT

In this thesis, it is aimed to explain the Design and Synthesis of Flame Retardant PS Electrospun Nanofibers. For this, various researchers of experts in the field were examined and the flame-retardant to nanofibers was observed in the laboratory environment. As a result of this thesis, it is aimed to prove that the nanofiber has a high flame retardancy resistance.

SYMBOLS

cm : Centimeter

gr : Gram

mm : Millimeter

TiO_2 : Titanium Dioxide

% : Percentage

ABBREVIATIONS

ASTM: American Society for Testing and Materials

DMF : Dimethylformamide

FTIR : Fourier Transform Infrared Spectroscopy

FT-IR : Fourier Transform Infrared Spectroscopy

IEC : International Electrotechnical Commission

IR : Infrared Spectroscopy

PS : Polystyrene

UL94 : Underwriters Laboratories 94

ZB : Zinc Borate

LIST OF FIGURES

PAGE

LIST OF TABLES

PAGE

1. INTRODUCTION

Electrospinning is a simple and effective method to produce ultrafine fibers with diameters ranging from nanometers to micrometers. Liquid solution molecules, which are positively or negatively charged by being exposed to a strong electric field, try to move away from each other, just as the similar ends of two magnets repel each other. This repulsion causes the liquid to take the form of a water droplet in the direction of the electric field. However, the pushing force reaches such a point that the liquid drop elongates and becomes thinner, just like a piece of gum. The solution, which dries as it travels through the air, accumulates on a counter plate as continuous filamentous fibers, just like a thawed ball of wool. With this method, it is possible to obtain nano-sized filamentous structures that are 20,000 times thinner than a human hair (in micron size). The resulting fibers can have a wide range of applications, including tissue engineering, drug delivery, and filtration.

1.1. General Information

The electrospinning technique, which was founded in the early 16th century by the English physicist William Gilbert, electrostatically charged amber dissolved in water and sprayed it on the counter surface in pieces from a conical needle tip, was patented by J. F. Cooley and W. J. Morton in the early 1900s and has been since then. managed to attract the attention of researchers in the field of biomedicine. The technique, which was first envisaged to be used to obtain filamentous structures in the field of textiles in the 1930s, then spread to other material areas, especially in the 1990s, when nanotechnology began to make a name for itself. (Tucker, 2012)

Today, ceramic, polymer and composite nanofibers and nanotubes are considered as the most attractive materials in nanotechnology. Due to their small size and large surface area, they provide unique mechanical, optical, electronic, magnetic, and chemical properties for a variety of applications. Electrospinning method has been widely used in the production of nano-sized fibers in recent years.

Electrospinning method mainly consists of three main parts (Syringe pump, collector, and high voltage power supply). Two different types of electrospinning devices are given below.

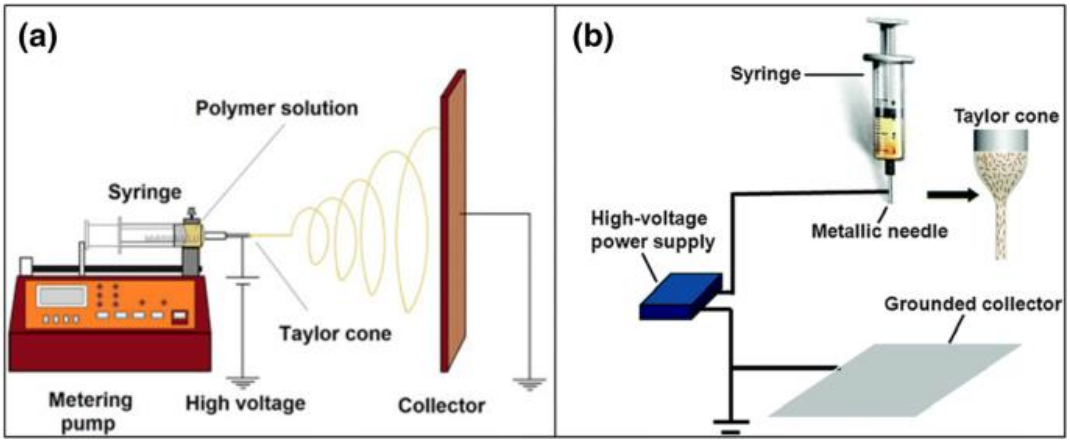

Figure 1.1. Simulation of electrospinning (Chinnapan, Krishnaswamy, Xu, & Hoque, 2022)

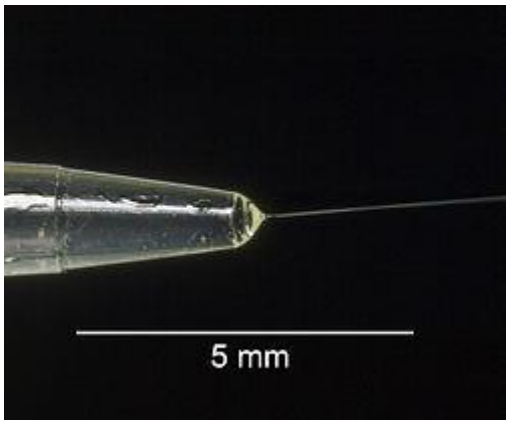

Figure 1.2. Needle point

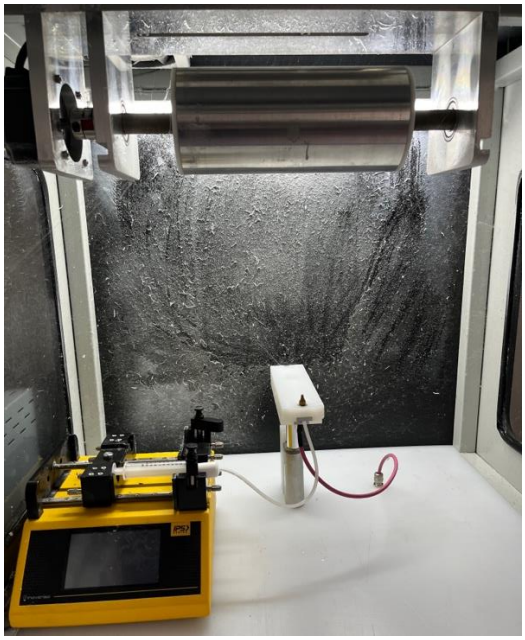

Figure 1.3. Electrospun nanofibers production setup

While a single solution is used in electrospinning processes, in some cases different solutions can be used together to achieve results that can achieve certain goals.

Many variables affect the solution to nanofiber transformation by electrospinning. (Doustgani, Vasheghani-Farahani, Soleimani B, & Hashemi-Najafabadi, 2012)

These:

- Molecular weight
- Polymer structure (straight, branched, network)
- Viscosity
- Surface tension
- Conductivity
- pH

In addition, the process parameters will also affect the result. These are:

- Voltage
- Distance between the collector plate and the needle

• Concentration of solution

• Flow rate

1.1.1. Concentration Effects

Considering the relationship between concentration and strength, it was observed that even though there was an increase in strength with the increase in the concentration ratio, the strength value decreased after a certain point with the increase in the concentration ratio. That is, an optimum value was reached, and the strength value started to decrease again after that point.

When the module value is examined, a linear increase was observed with the increase in concentration.

1.1.2. Voltage Effects

A linear increase was observed in both the strength and modulus values with the increase in voltage.

1.1.3. Distance

A linear decrease was observed in both strength and modulus values with increasing distance. Shorter spinning distance resulted in stronger fiber formation.

1.1.4. Flow Rate

Flow rate did not have significant effect on the mechanical properties of the fibers.

1.2. Literature Review

First of all, a literature review was conducted to gather general information about electrospinning and to have information about nanofiber production. In return, the information obtained was summarized and the research for the experimental phase was continued. Research has been done on how to resist flame resistance for PS, what stages it will go through and how to produce it. It was investigated what tests could be applied for the nanofibers produced and how the test would be applied for the flame-retardant.

1.2.1. Electrospun Nanofiber Production Stage

In order to be suitable for the purpose of this study, the selection of the components that will form the nanofibers was decided by examining the previous studies.

DMF is one of the polar solvents and is used for dissolving many polymers, including PS. Due to its molecular structure, DMF weakens the interactions between the polymer chains, facilitating and accelerating the dissolution process. In terms of this characteristic, DMF is a good choice for dissolving PS. However, due to its high volatility, it is important to strictly adhere to occupational health and safety measures when working with DMF to avoid any negative impact on human health. (Toy, 2003)

DMF is an effective solvent for many polymers, but it also poses a risk of interacting with certain substances. However, the combination of DMF and PS is a compatible pair in this regard.

TiO_2 is a high thermal stability material. it strengthens high temperature resistance and thermal stability in nanofibers to which it is added. (Madani, ve diğerleri, 2013). Generally, the thermal resistance capacity is high at high temperatures (up to 1000^o) and the thermal degradation rate is low.

Although zinc borate is not as durable as TiO_2, it can be strong and stable against thermal resistance up to certain temperatures (up to 400^o-500^o). Due to the differences these two substances have, their usage areas may vary.

2. EXPERIMENT

2.1. Materials

Polystyrene (ALDRICH Chemistry) was used in this study. DMF (dimethylformamide) was used as the solvent. In this experiment, a total of 6 solutions were prepared and nanofibers were produced. Polystyrene purchased from (ALDRICH Kimya) and DMF purchased from (EMSURE). The chemicals used to compare with polystyrene and obtain the combustion resistance we want are Zinc Borate (ZB) and Titanium Dioxide (TiO2). Zinc Borate purchased from (REFSAN).

2.2. Preparation of Spinning Solution

PS solutions were prepared in 6 different ways. The DMF ratio was kept constant at all times and in each solution. The general solution was 20 grams in total and mixed all with 16 grams of DMF solvent. The fraction changed in subsequent solutions was percentages in 4 grams. Examples of solutions prepared can be seen in Figure 2.1.

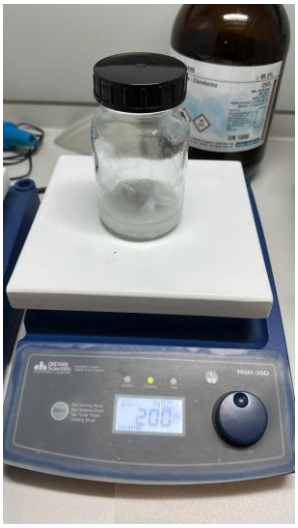

Figure 2.1. Dissolving operation of solution

While these solutions were being prepared, they were carried out in a very meticulous and clean manner, following the necessary laboratory rules. The brand and model of the device left to dissolve the solutions is Daihan Scientific MSH-20. The mixer machine was operated at a temperature of 200 rpm and 45 degrees. These conditions applied to all solutions and were made under the same conditions. The image of the device used is in Figure 2.1.

The first solution was prepared with Pure 75% DMF and 25% PS. The second solution has the same DMF content, while PS and Zinc Borate are 85% and 15% respectively. The third solution was prepared as 90% PS and 10% ZB. The 4th solution is 95% PS and 5% ZB. Titanium Dioxide was used in the last two solutions, as it was thought to further strengthen the fire resistance. In solution 5, it was prepared by mixing 85% Polystyrene with 7.5% ZB and 7.5% TiO2. In the 6th and last solution, only 85% PS and 15% TiO2 were mixed and the solution preparation stage was completed in this way. In order to understand the prepared solutions more clearly, they are summarized in tabular form. The ratio of solutions can be seen in Table 2.1.

Table 2.1. The content of the prepared results

Solutions	**Samples**	**DMF (gr)**	**PS (gr)**	**Zinc Borate (gr)**	**TiO_2 (gr)**
1	Pure	16	4 (100%)	0 (0%)	0 (0%)
2	5% ZB	16	3.8 (95%)	0.2 (5%)	0 (0%)
3	10% ZB	16	3.6 (90%)	0.4 (10%)	0 (0%)
4	15% ZB	16	3.4 (85%)	0.6 (15%)	0 (0%)
5	7.5% ZB 7.5%TiO_2	16	3.4 (85%)	0.3 (7.5%)	0.3 (7.5%)
6	15% TiO_2	16	3.4 (85%)	0 (0%)	0.6 (15%)

2.3. Electrospinning Process

The electrospinning assembly is shown in Figure 2.2. The images of the syringe and the pump machine used in the electrospinning process are in Figure 2.2. Before starting the electrospinning process, the solutions were rested for about half an hour. The reason for this was because the solution was desired to stagnate a little. During this rest period, the syringe and pipette were prepared and the electrospinning device was cleaned. We covered the drum with greaseproof paper so that our nanofiber could be collected. Then the solution was carefully drawn into the syringe, the pieces were placed and placed

in our pump machine. The other end of the plastic was also attached to the needle. The used parameters were entered into the electrospinning device and the solutions were run.

Figure 2.2. Syringe pump and electrospinning machine

There were parameters used during electrospinning. Values such as voltage and flow were the same in all but the last solution. In all solutions, the drum was adjusted to 500 rpm and was never changed. This was his optimum level. The distance between the needle and the drum was 25 cm and this was not changed. All experiments were done in the same way. The voltage value was the same in all solutions. It is set to 25V. One of the nanofiber samples obtained can be seen in Figure 2.3.

Figure 2.3. Sample of electrospun nanofiber

3. TESTS AND RESULTS

3.1. FTIR Test

3.1.1. General Information

FTIR is a fast, reliable, precise and inexpensive technique that can be used to characterize the chemical composition of various microorganisms (R., 2011). FTIR is a fast, reliable, precise and inexpensive technique that can be used to characterize the chemical composition of various microorganisms (Ergin, et al., 2013).

FTIR analysis is an analysis method that examines the infrared light spectrum of a substance. This analysis method is used to determine the bonds between the materials used, to determine how good the components are and to analyze different substances.

An infrared spectroscopy device basically consists of three parts: the light (IR) source, the interferometer and the detector. In addition to these, there are parts of the computer where the beam splitter, the sample is loaded and the computer parts where the data is processed (Figure 3.1.).

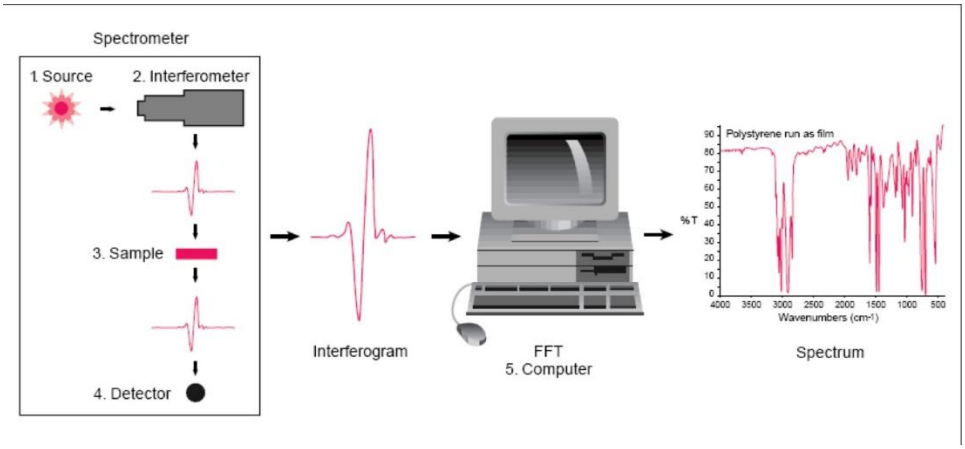

Figure 3.1. Essential parts of a representative FTIR system

IR light is sent to the sample to obtain an IR spectrum. In order for a molecule to absorb IR light, there must be a net change in the molecule's natural dipole moment as a result of the molecule's vibration. It is looked at how much of the light transmitted to the sample is absorbed at a certain energy. The energy from which a signal is obtained in the absorption spectrum gives the vibrational frequency of the sample molecule (Toyran, 2008).

Since information is accessed directly at the atomic level with FT-IR, even very small changes in molecules can be detected. Certain molecules are characterized by molecular bond vibration signals at certain frequencies (cm-1) when exposed to infrared light. Changes in different conditions over these signals can be easily monitored by FT-IR.

3.1.2. Preparation of FTIR Test

An FTIR spectrometer is used for FTIR analysis. In essence, the recorded absorption spectrum is the result of the interaction between infrared radiation and the sample. It can also briefly mention the stages of this analysis. First of all, while preparing the samples, they were cut in 2cmx2cm dimensions and since the samples were solid, it would have been sufficient to cover a small area where the analysis would be done. Then, before performing this analysis, the analysis area was cleaned with a special liquid. Then the test was done blank first. The reason for this was not to disturb the sensitivity due to the weather and to ensure that the measurements gave the most accurate result. After the background measurement is complete, the spectrum of the sample is taken and infrared light is sent to the sample and absorption occurs when it combines with the sample. The obtained results were made suitable for data analysis with the help of a computer program. Data were taken as wavenumber and wavelength. Data were then recorded for comparison and interpretation with general polystyrene, zinc borate and titanium dioxide. In this FTIR analysis, the machine we used was the PerkinElmer precisely Spectrum 100 FT-IR Spectrometer. We can see the visuals of the machine we use and our sample test phase in Figure 3.2.

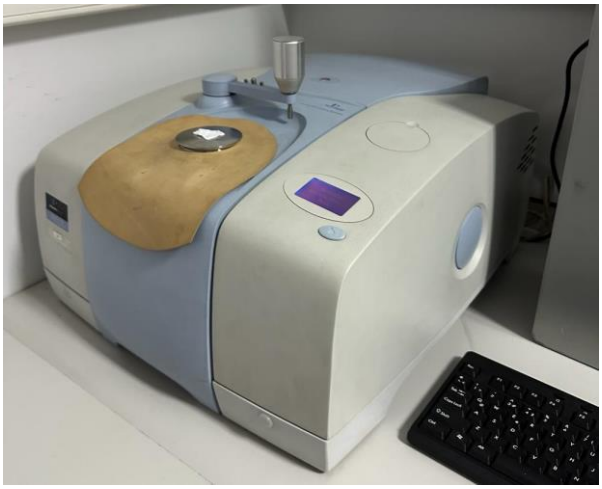

Figure 3.2. FTIR device

3.1.3. FTIR Spectra of Pure Polystyrene

The FTIR analysis for the first prepared nanofiber, Pure polystyrene, can be seen below. Polystyrene results from reference articles were used for comparison.

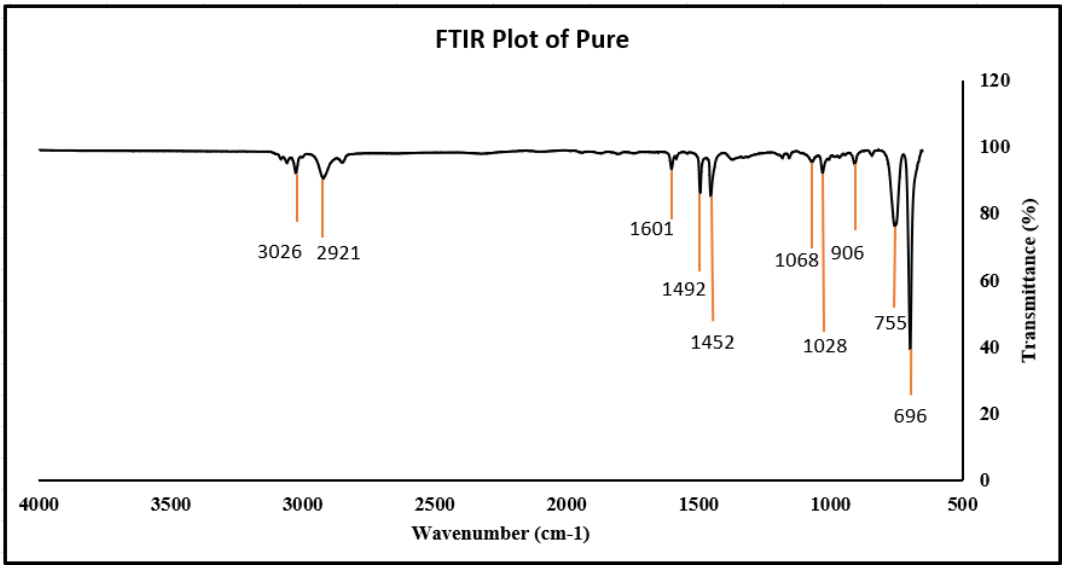

Figure 3.3. FT-IR spectra of electrospun pure polystyrene fibers

3.1.4. FTIR Spectra of Polystyrene With 5% Zinc Borate

The FTIR analysis for the prepared second nanofiber, 5% ZB polystyrene, can be seen below. Here, the results of the FTIR analysis of zinc borate examined from reference articles were evaluated.

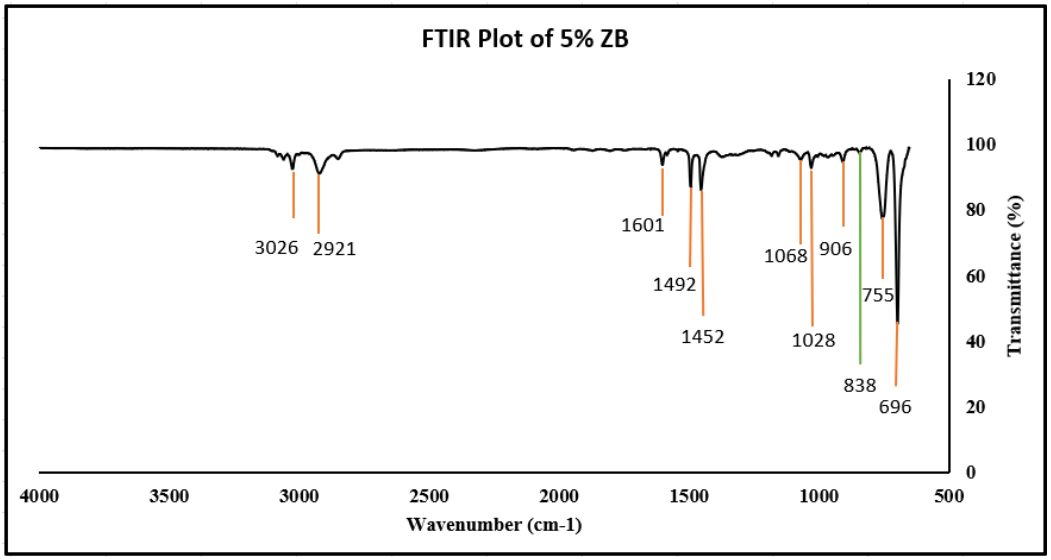

Figure 3.4. FT-IR spectra of electrospun 5% ZB polystyrene fibers

3.1.5. FTIR Spectra of Polystyrene With 10% Zinc Borate

The FTIR analysis for 10% ZB polystyrene, the third nanofiber prepared, can be seen below. Here, the results of the FTIR analysis of zinc borate examined from reference articles were evaluated.

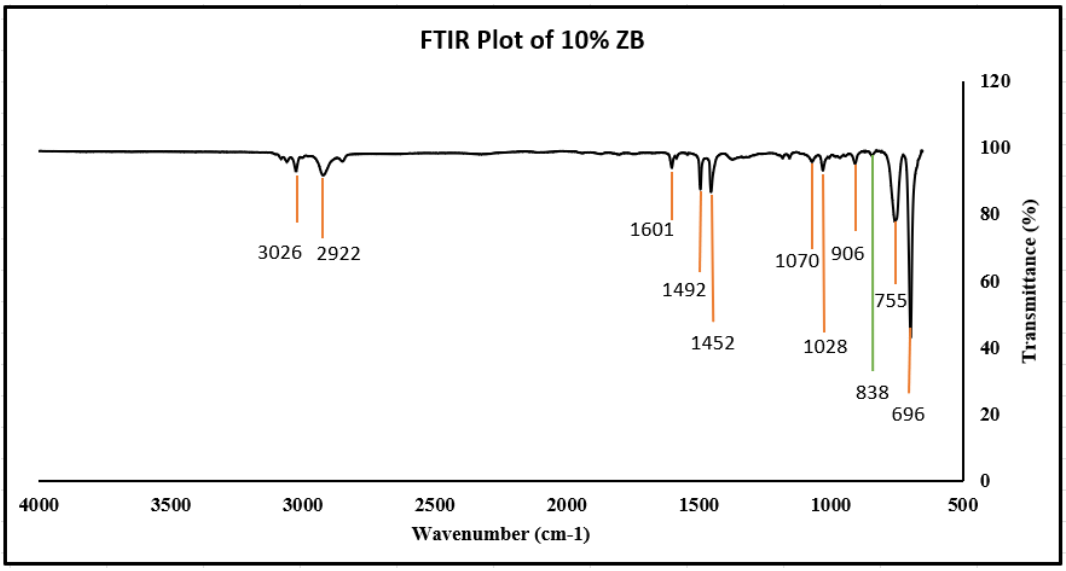

Figure 3.5. FT-IR spectra of electrospun 10% ZB polystyrene fibers

3.1.6. FTIR Spectra of Polystyrene With 15% Zinc Borate

The FTIR analysis for 15% ZB polystyrene, the 4th nanofiber, can be seen below. Here, the results of the FTIR analysis of zinc borate examined from reference articles were evaluated.

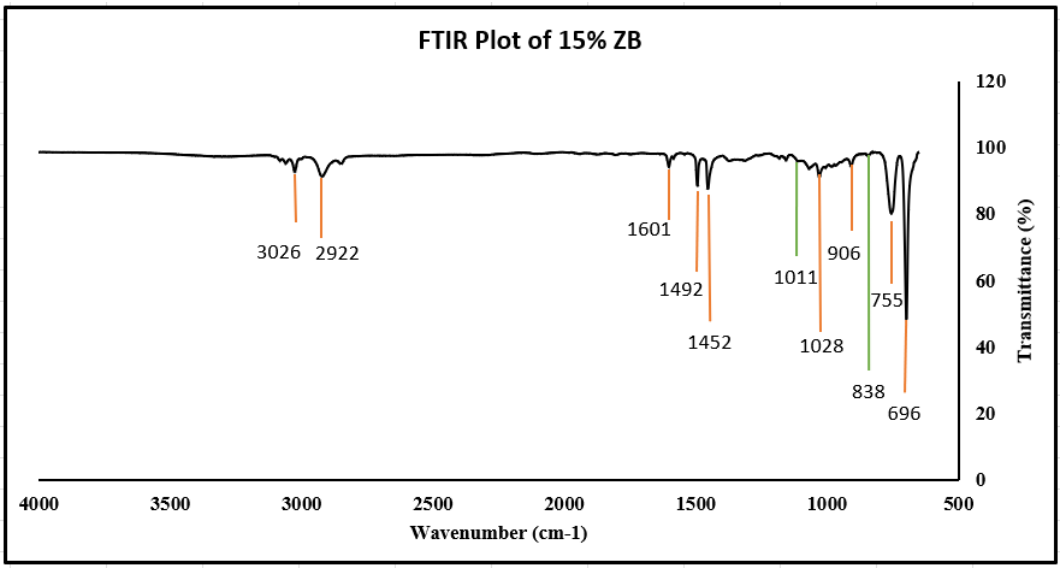

Figure 3.6. FT-IR spectra of electrospun 15% ZB polystyrene fibers

3.1.7. FTIR Spectra of Polystyrene With 7.5% Zinc Borate And 7.5% TiO_2

We can see the FTIR analysis for polystyrene with 7.5% ZB and 7.5% TiO_2, the 5^{th} nanofiber we prepared, below. Here, we had the chance to evaluate the results of FTIR analysis of zinc borate and TiO_2 that we investigated from our reference articles.

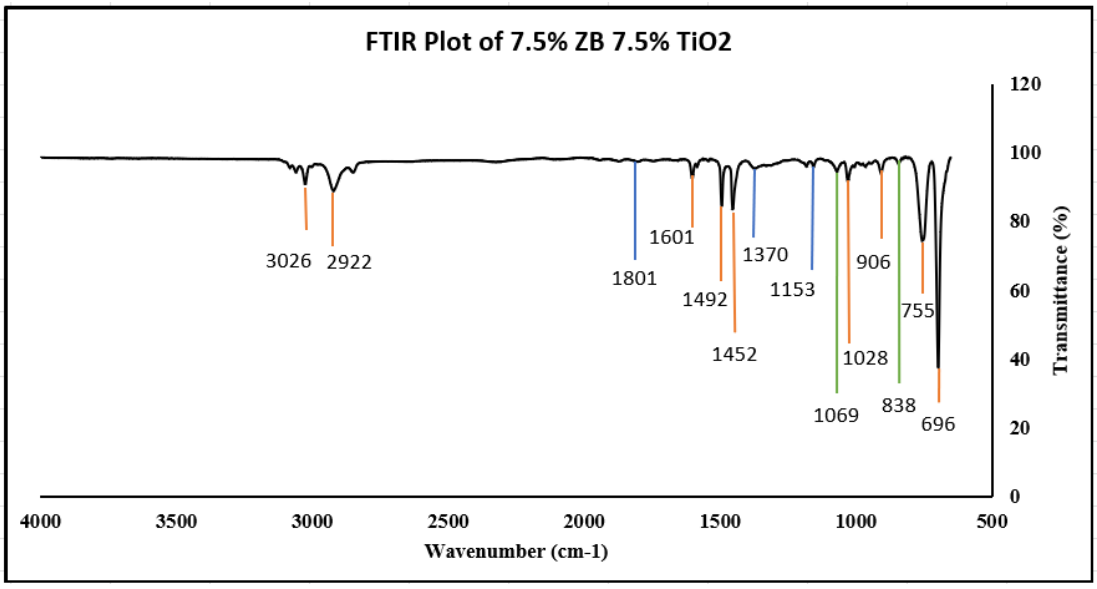

Figure 3.7. FT-IR spectra of electrospun 7.5% ZB and 7.5% TiO2 polystyrene fibers

3.1.8. FTIR Spectra of Polystyrene With 15% TiO_2

The FTIR analysis for polystyrene containing 15% TiO_2, the 6th nanofiber, can be seen below. Here we had the chance to evaluate the results of the TiO_2 FTIR analysis, which we reviewed from our reference articles.

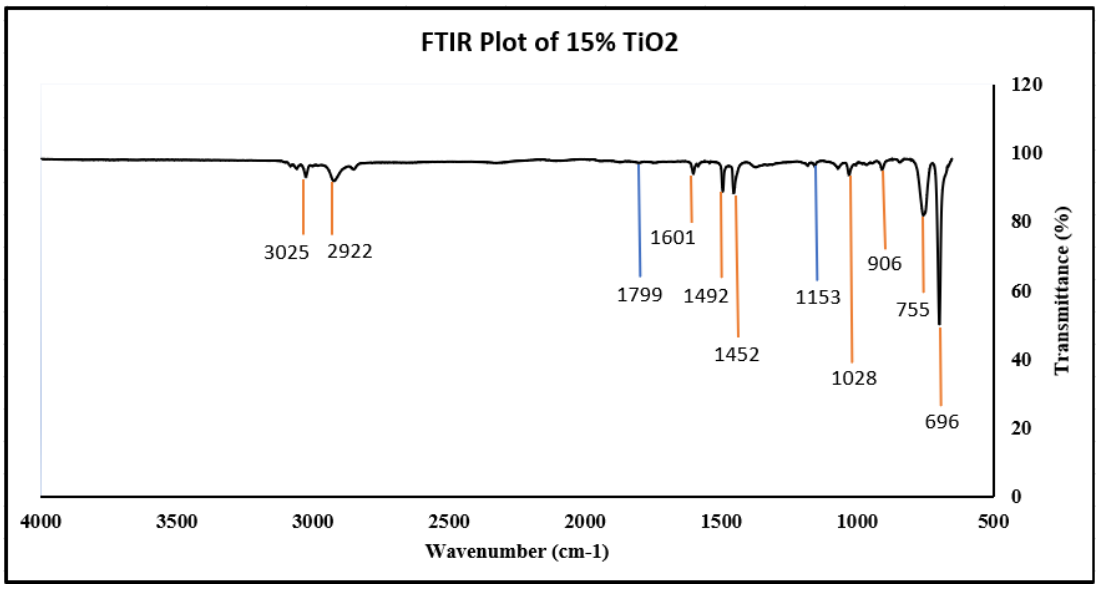

Figure 3.8. FT-IR spectra of electrospun 15% TiO2 polystyrene fibers

3.1.9. FTIR Spectra of All Of Them In One

All the obtained results were collected on one graph for easy comparison. The results obtained can be seen collectively in Figure 3.9.

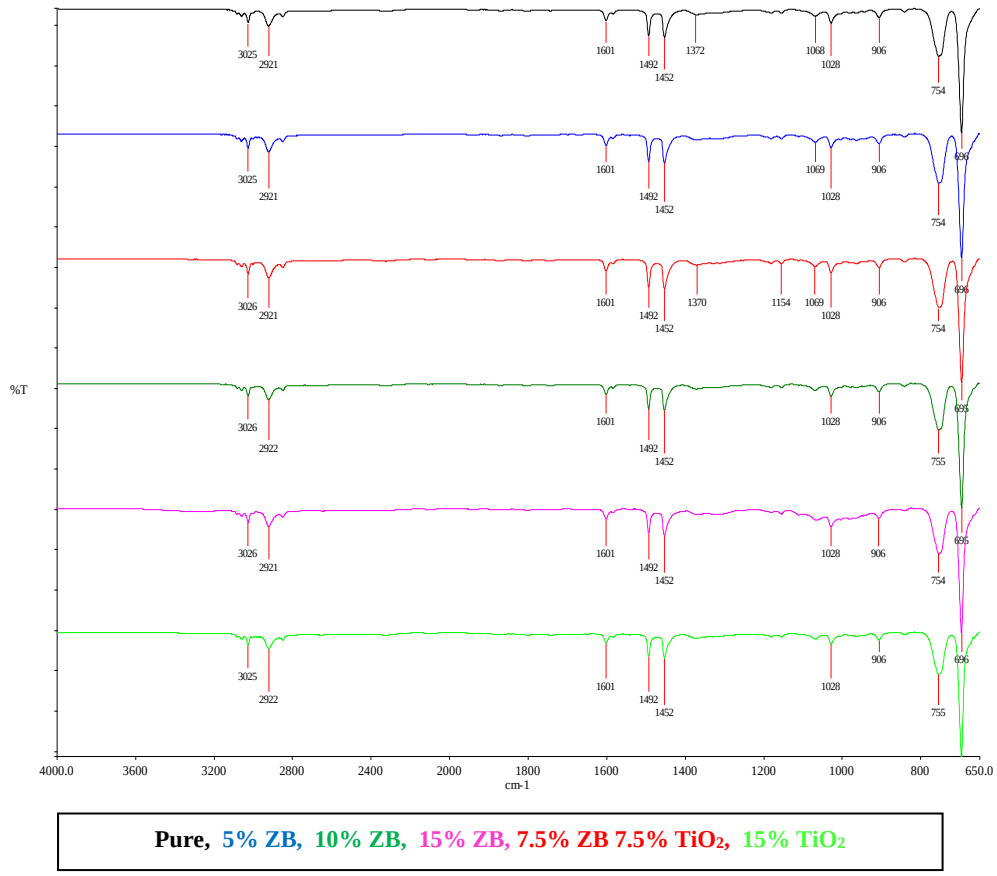

Figure 3.9. Diagram with FTIR results for all samples

3.2. Contact Angle

The contact angle is the angle formed at the moment of interaction between liquids and solid surfaces. This angle also explains the slope of the liquid on the solid surface and the spread or accumulation of the liquid above the surface. This angle also explains the slope of the liquid on the solid surface and the spread or accumulation of the liquid above the surface. The behavior of the liquid on the solid surface is affected by these factors.

The interaction on the liquid and solid surface is affected by these factors. The spread or accumulation of liquid on a surface is associated with the magnitude of this contact angle that occurs between the liquid and the solid surface. A higher contact angle means that the accumulation of fluid is high, while a lower contact angle means that the propagation is higher.

If the liquid is spreading over a solid surface, the contact angle is usually small. In this case, it is observed that liquid molecules spread out on the solid surface, forming a layer. This propagation usually occurs on homogeneous and flat solid surfaces and forms a contact opening. For example, a drop of water shows an excellent spreading and wetting property on a glass surface, creating a contact angle close to 0 degrees. Glass is structurally hydrophilic and attracts water molecules well, allowing it to adhere and spread. It should be kept in mind that when performing experimental measurements or the conditions of the experimental environment, there may be differences in the measurement values.

In contrast to these hydrophilic substances, there are also hydrophobic substances and water tends to accumulate on the surface when it comes into contact with these substances. In these cases, the contact angle shows high values. For example, when mercury drops come into contact with the glass surface, the contact angle is about 150. On hydrophobic surfaces, water molecules collect and form droplets and interact weakly with the surface. This indicates the tendency of the liquid to escape from the solid surface.

The contact angle is important in surface coating works, technological developments, material selection, device designs and many other areas. In addition, the contact angle value plays a major role in microelectronic device production, painting and coating works, surface cleaning processes.

Contact angles differ in many liquid-solid binaries. In these different situations, contact angle measurement is important to determine the properties of substances.

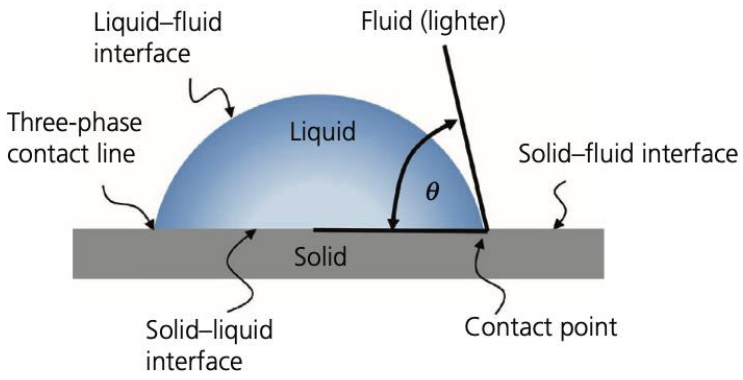

Figure 3.10. The contact angle q is shown for a sessile drop. (Volpe, Siboni, Amirfazli, Jaroslaw, & Marmur, 2017)

Hydrophobic materials have low wetting ability. On the contrary, hydrophilic substances are substances with high wetting ability. Wettability is a term that tries to express the amount of diffusion and accumulation of water on the surface. The contact angle is used to describe the surface behavior of the produced nanofibers in terms of hydrophilicity or hydrophobicity (Ray, et al., 2018).

For water, the contact angle on hydrophilic surfaces is expected to be less than 90°.On hydrophobic surfaces, values equal to or higher than 90° are expected.

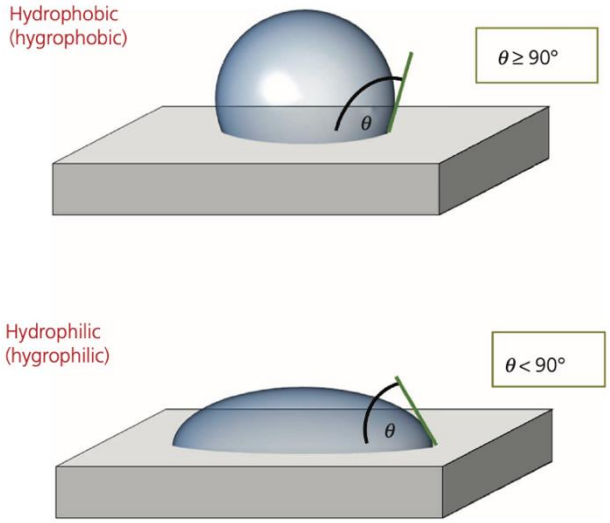

Figure 3.11. Liquid drops on a hydrophobic surface and a hydrophilic surface

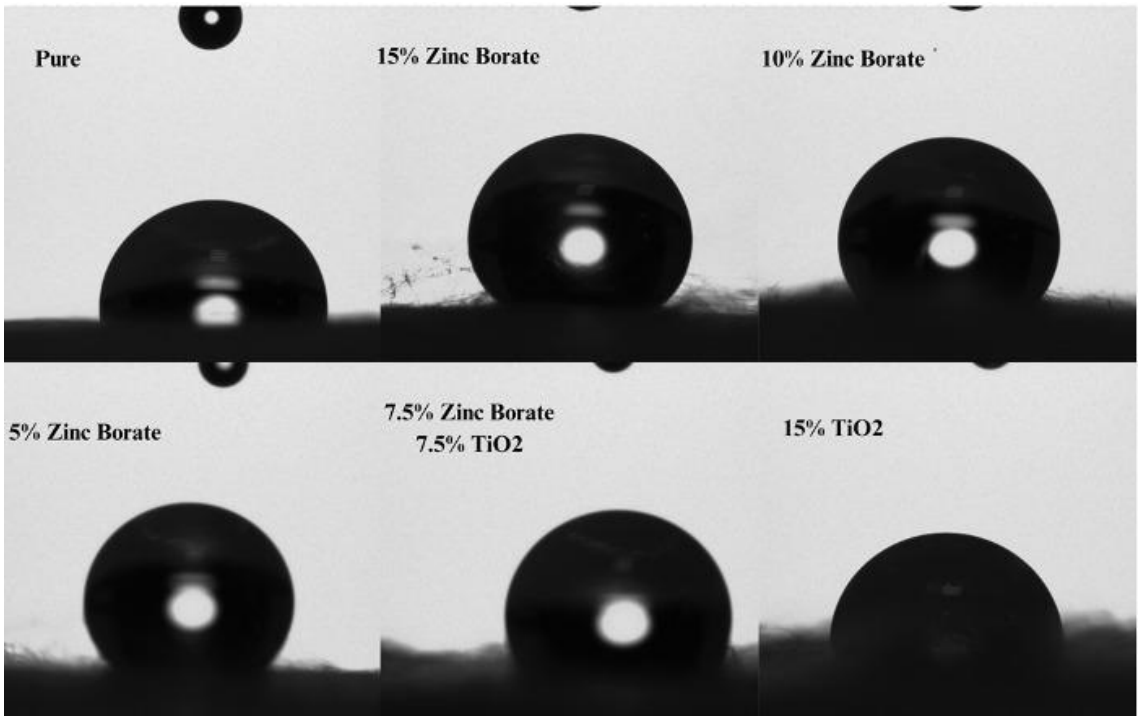

Figure 3.12. Images of measuring contact angles

Table 3.1. Contact angle values of the samples

No	Samples	Drop 1	Drop 2	Drop 3	Mean	Standard Error
1	Pure	98.68°	102.14°	93.3°	98.04°	2.57
2	5% ZB	123.24°	110.25°	125.24°	119.58°	4.70
3	10% ZB	105.43°	117.71°	96.58°	106.57°	6.13
4	15% ZB	103.14°	127.37°	126.99°	119.17°	8.01
5	7.5% 7.5% ZB	106.86°	97.08°	104.23°	102.72°	2.92
6	15% TiO2	85.13°	78.43°	85.01°	82.86°	2.21

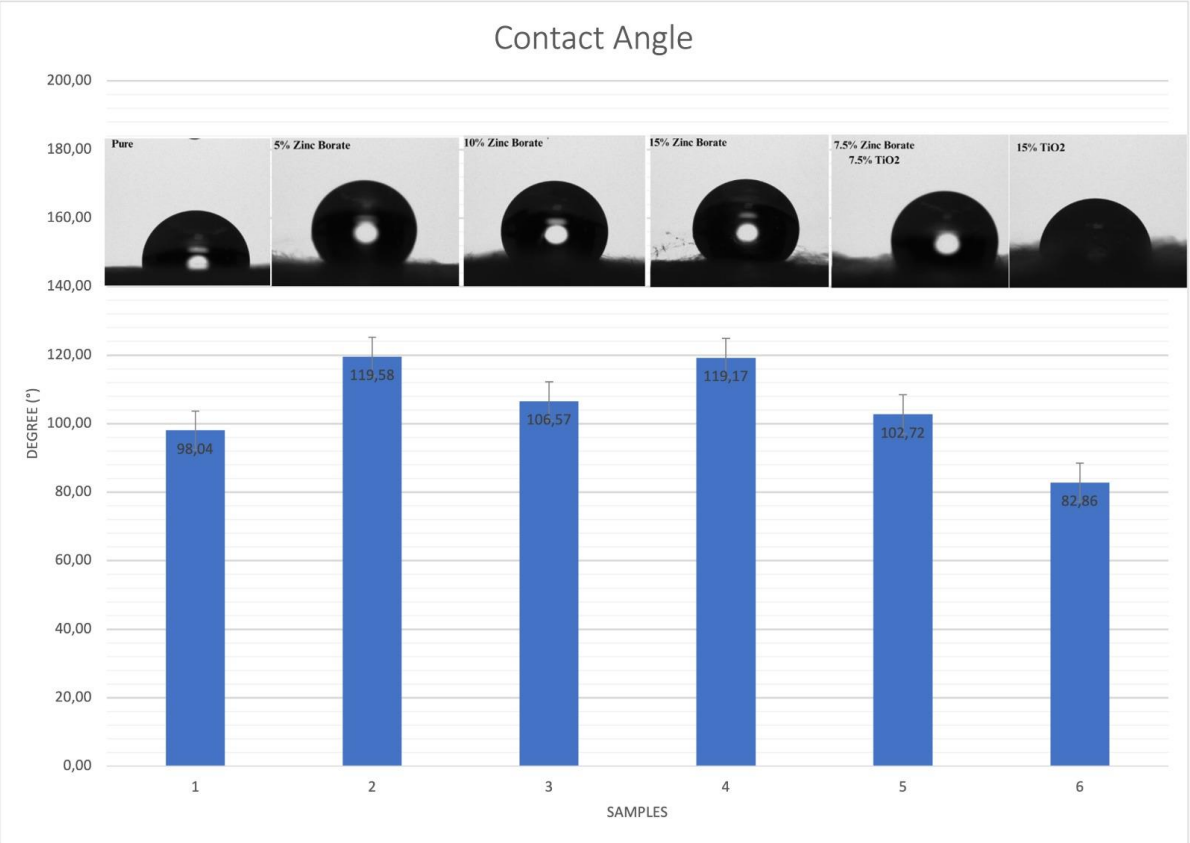

Figure 3.13. Contact angle for samples (error bars are based on standard errors from three replicate tests)

Table 3.2. Hydrophilic/hydrophobic situations of samples

No	Samples	Hydrophilic/Hydrophobic
1	Pure	Hydrophobic
2	5% ZB	Hydrophobic
3	10% ZB	Hydrophobic
4	15% ZB	Hydrophobic
5	7.5% 7.5% ZB TiO2	Hydrophobic
6	15% TiO2	Hydrophilic

3.3. Flame-Retardant Test

3.3.1. General Information for Flame-Retardant Tests

The flame retardancy test is of great importance in determining the fire resistance of the material and controlling the fire safety standards. In this test, the burning properties of materials, especially the spread of the flame, the dissipation of heat, the formation of smoke and the post-burning state, are examined. It is applied in various materials such as plastics, building materials, textile products and electrical cables, while it can also be used for the electrospun nanofiber materials produced.

In UL94 type combustion tests, evaluations are made by monitoring the combustion behavior of plastics and their derivatives. A sample taken in the UL94 type test is exposed to the ignition source for a certain period of time and the flame spread and speed, burning time and self-extinguishing time after burning are examined. In summary, this test is used to observe how the material behaves during a fire and to what extent it prevents the spread of flames.

There are 3 parts to UL94 standards. The terms of this section are given below.

Flame test criteria per UL 94 VTM (thin material vertical burning test)

Test Criteria	VTM-0	VTM-1	VTM-2
Total Burning time of each test specimen(s)	≤ 10	≤ 30	≤ 30
Dripping of burning specimens	No	No	Yes
Specimen completely burned	No	No	No

Figure 3.14. UL94 standards (Baddam, Ijaola, & Asmatulu, 2021)

Another type of test, the ASTM E84 test, examines the combustion behavior of construction materials. Samples are prepared from materials used in processes such as wall and ceiling coverings and left to the ignition source for a certain period of time to measure the rate of flame spread, smoke formation and smoke spread. This test is important to evaluate the fire resistance of construction materials and the properties of smoke produced during a fire.

The IEC 60332 test, on the other hand, examines the combustion properties of electrical cables. In this test, a cable is used as a sample and in the same way, it is contacted with a flame source for a certain period of time. This test is of great importance

to evaluate the reactions of electrical cables used in daily life during fire and to take precautions.

Flame retardancy tests are not only sufficient to examine the fire safety situation, but also provide great benefits by using them in increasing the reliability of the materials and in the development stages. These tests are considered an important factor in terms of human safety and health by providing benefits in firefighting and prevention processes.

3.3.2. Preparation To Flame Retardant Test

The samples of fiber, produced in the dimensions of 12.5x1.5, were prepared for a flame retardancy test. The aim was to observe the extent of flame spread on the sample by igniting it with a vertically positioned ignition source. Additionally, the occurrence of dripping during combustion is crucial for the test.

Self-extinguishing after ignition is important according to the UL94 standard. Among these results, measuring the extinguishing time is crucial for determining the classification within the UL94 standard.

Table 3.3. Flame retardant test results and calculation of three replicate tests

No of Samples	Final Length 1 (cm)	Final Length 2 (cm)	Final Length 3 (cm)	Mean (cm)	Error	Loss%
1	4.62	4.98	5.35	4.98	0.21	60.2%
2	5.28	5.43	5.83	5.51	0.16	55.9%
3	6.76	6.35	7.22	6.78	0.25	45.8%
4	7.65	8.44	7.76	7.95	0.25	36.4%
5	10.12	9.96	9.38	9.82	0.22	21.4%
6	10.18	10.13	10.98	10.43	0.27	16.6%

In the flame-retardant test, each sample size was prepared as 12.5cmx1.5cm. 3 of these samples were prepared. In this test, each sample was tested as in Figure 3.15. Once the burning was complete, the final lengths of each sample were measured to see how long they lasted. After these lengths were noted, the average of all 3 tests was taken and added to the table. According to these averages, error and percentage loss were calculated. These results can be seen in Table 3.3.

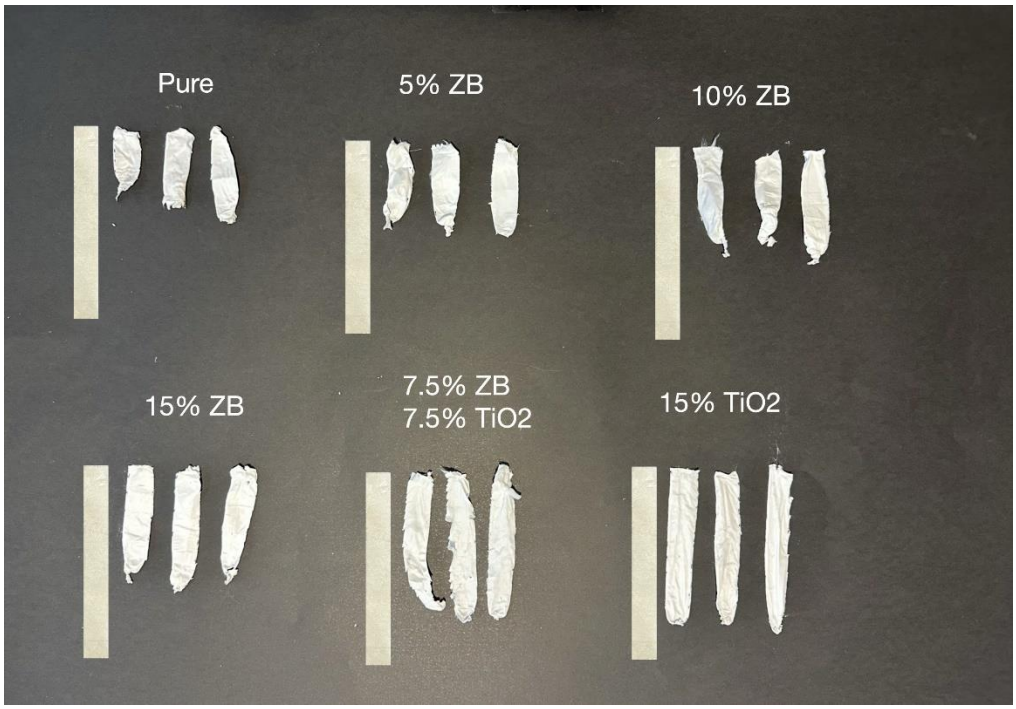

Figure 3.15. Initial and final lengths of samples of three replicate tests

Figure 3.16. An example from the flame-retardant test moment

Table 3.4. Suitability table with UL94 V0 standards

Samples	Dripping	Self-Extinguishing Time	Burning up to holding clamp
Pure	No	≤10s	No
5% Zinc Borate	No	≤10s	No
10% Zinc Borate	No	≤10s	No
15% Zinc Borate	No	≤10s	No
7.5%- 7.5% Zinc Borate and TiO2	No	≤10s	No
15% TiO2	No	≤10s	No

4. COST ANALYSIS

Table 4.1. Cost of Experiment Materials

Experiment Materials (100gr)	**Cost ($)**
Polystyrene	0.15
Dimethylformamide	2.57
Titanium Dioxide	1.52
Zinc Borate	3.07
Sterile Pipette (for 6 pieces)	1.85
Plastic Syringe (for 6 pieces)	2.00
Greaseproof Paper (for 6 pieces)	0.60
Flame Source (for 1 pieces)	1.00
Energy (Electric)	2.00
Total Cost	**14.76**

Table 4.2. Cost of Equipment Rental

Equipment Rental	**Cost ($)**
Electrospinning Device	0
Mixer Machine	0
Laboratory Equipment	0
Total Cost	**0**

Table 4.3. Cost of Tests

Tests	**Cost ($)**
FTIR Analysis	0
Contact Angle Analysis	0
Flame-Retardant Analysis	3.25
Tools	3.85
Total Cost	**7.1**

Cost analysis is the process of evaluating and recording the costs related to this process during a project, work and production. Expenditures are classified under certain

headings and noted transparently. In this process, material, employee, equipment fees are added to this account. The cost of each project is unique.

Cost analysis is an important topic that should be included in the studies because it can give an idea about the feasibility and profitability of a project. It has a great impact on effective budget management and provides a perspective on the continuation of the work.

The materials required for this study, the materials used, the equipment, the laboratory services, etc. expenses are given in the tables above. These tables categorized the cost account of this study by showing it under different headings.

The most important materials to be used in the study are polymers and solvents. The polymers and solvents used here are shown in the cost analysis table. The most important issue in the electrospinning process is the supply of the electrospinning device. Although rental services were provided for the use of the device, no rental was made in this study and it was provided to be used free of charge during the study. With the agreement, the laboratory with electrospinning device was rented free of charge to be used for studies.

Many disposable materials used in the study were added to the cost calculation. However, auxiliary equipment available in the laboratory environment is not included in this calculation. The total cost of this study is $21.86.

5. DISCUSSION

5.1. Explication of FTIR Analysis

The PerkinElmer Spectrum 100 Series was used during this test phase and the results can be seen above. According to the results in the FTIR test, nanofiber result No. 1 was compared with other nanofiber results. According to these comparisons, zinc borate effects were observed through green peaks. TiO_2 effects were also seen through blue peaks.

The aim of this test was to observe that the chemicals bonded with each other and dissolved well. Although the observations made cannot be taken even if the peaks are not very clear, it is observed that ZB and TiO_2 form bonds through the small peaks seen. Success in this test was very important for flame-retardant. In order to get accurate results in flame resistance, this test had to be observed first. At this point, good dissolution of the mixtures was important to increase the durability of the nanofibers and to obtain more accurate and clear results. At this point, good dissolution of the mixtures was important to increase the durability of the nanofibers and to obtain more accurate and clear results. As a result, the results obtained here were a light for the flame-retardant and it was observed that it could be successful.

5.2. Explication of Contact Angle Results

According to the data obtained, the contact angle value of 5 of the samples exceeded 90 degrees, while the contact angle value of 1 of them remained below 90 degrees. Accordingly, 5 samples were observed to comply with the hydrophobic standard while 1 sample complied with the hydrophilic standard.

Based on these results, it can be inferred that when zinc borate is added to the pure solution, it increases the contact angle, thus strengthening its hydrophobic state.

When comparing the results of sample number 5 and the results of the previous 4 samples the addition of TiO2 to the mixture appears to weaken the hydrophobicity of the resulting nanofiber. Likewise, the increased TiO_2 ratio of sample 6 compared to other samples confirmed that it increased its hydrophobicity. In addition, according to the results of samples 1 and 6, the addition of TiO_2 was observed to move from the hydrophobic state to the hydrophilic state.

5.3. Explication of Flame-Retardant Results

In the flame-retardant test, the burning behavior was examined by igniting the samples once. For each sample, this test was repeated 3 times. According to the results, it is seen that the sample numbers 1 and 2 give the most loss once burned. Of these two samples, one was pure and the other had a zinc borate content of 5%, which was expected to yield the most losses. Samples 3 and 4, with the highest zinc borate ratios, show a loss of about 45.8% and 36.4%, respectively. When zinc borate increased the ratio in the mixture, its flame resistance increased and no flame appeared. When the ratio of zinc borate in the mixture was increased, the flame resistance increased and the flame self-extinguished. Since TiO_2 was added to nanofibers 5 and 6, it was expected to have higher flame resistance. According to the results, a loss of 21.4% was observed in sample number 5 and 16.6% in sample number 6. According to these data, maximum flame resistance was observed in these two samples. The flame resistance of titanium dioxide has been theoretically and experimentally proven and studied.

The results prepared according to the UL94-V0 standards, which we have taken as a reference in Figure 3.15., are shown in Table 3.4. Drip was not observed in the flame-retardant test of the samples used for the test. From this point of view, since the flame is self-dampening in all of the samples, interpretations can be made about the burning resistance by looking at the percentage losses. Looking at the losses by mass, the addition of ZB increased the fire resistance of the electrospun nanofiber, while the addition of TiO_2 further strengthened the fire resistance. The self-extinguishing time of the samples also complied with UL94-V0 standards, as it was less than 10 seconds.

6. CONCLUSION

For the purposes of this study, PS electrospun nanofiber was produced for flame resistance. First, the solution was prepared in 6 different ways. In these solutions in pure form there were solutions in different proportions of zinc borate and titanium dioxide. Using these solutions, nanofibers were produced every week and the nanofibers were preserved. Samples were then made available for the tests investigated in the literature review. Samples were prepared for the first test, FTIR analysis, and the results were obtained with the help of a computer program. In line with these results, the chemical bonds of the samples and the level at which the solutions were mixed were observed. In line with this result, it was seen that the appropriate environment was created to proceed to the second test. Samples were prepared in sufficient size for contact angle testing. In the Contact Angle test, the wettability of the samples was examined and all but one of our samples were observed to be hydrophobic. In this case, it was found that the samples we prepared were not easily wet. For the third and final test, flame-retardant, samples were prepared according to the standards we reference and the appropriate environment was created. The results of the flame-retardant test show that the nanofibers using TiO_2 provided the desired strength. In addition, the nanofiber using zinc borate also showed resistance to flame, but this strength was not as high as TiO_2.

Wettability is the term that refers to how much it spreads when it comes into contact with water or how well it absorbs water. Substances with a high wetting ability can easily absorb water and spread on the surface. There is an inverse proportion between hydrophobic and wetting state.

Hydrophobic substances can be used in different areas because they offer a wide range of uses. It can be used in the paint and coating industry as it will provide water repellent and stain repellent properties. In the same way, it can be preferred in automotive and metal coating areas. In the biomedical field, it can also be useful to use it in cleaning products, produced glass surfaces, electronic devices and clothing.

Resistance to burning is of great importance in many areas of life. As a result of this study, it has been observed that if the zinc borate and titanium dioxide duo are used in fiber production, it increases the resistance against burning. As a result, it is interpreted that electrospun nanofibers produced with these materials will be useful in all equipment

that will provide fire safety, in construction materials, in the electronics industry and in many areas to provide a more sheltered structure in space and aviation studies. As technology and studies in this field progress, it will be possible to use it in more different fields.

7. REFERENCE

Al-Kadhemy, M. F., Abaas, W. H., & Fakher, I. (2013). The Effect of Gamma Radiation on the FTIR Spectrum of Crystal Violet Doped Polystyrene Films .

Baddam, Y., Ijaola, A. O., & Asmatulu, E. (2021). Fabrication of flame-retardent and superhydrophobic electrospun nanofibers.

Can-Herrera, L. A., Oliva, A. I., Dzul-Cervantes, M. A., Pacheco-Salazar, O. F., & Cervantes-Uc, J. M. (2021). Morphological and Mechanical Properties of Electrospun Polycaprolactone Scaffolds: Effect of Applied Voltage.

Chinnapan, B. A., Krishnaswamy, M., Xu, H., & Hoque, M. E. (2022). Electrospinning of Biomedical Nanofibers/Nanomembranes: Effects of Process Parameters".

Demirel, R. B. (2016). Elektrocekim yontemi ile nanofiber uretimi ve uygulamaları.

Doustgani, A., Vasheghani-Farahani, E., Soleimani B, M., & Hashemi-Najafabadi, S. (2012). Optimizinf the mechanical properties of electrosspun polycaprolactone and nanohydroxyapatite composite nanofibers.

Ergin, Ç., M., İ., Y., G., Özel, M. Z., Çon, A. H., Kabay, N., . . . Döğen, A. (2013). Fourier transform infrared spectral evaluation for the differentiation of clinically relevant Trichophyton species.

Ghosala, K., Agatemorb, C., Spitalskyc, Z., Thomasd, S., & Knye, E. (2019). Electrospinning tissue engineering and wound dressing scaffolds from polymer-titanium dioxide nanocomposites.

He, J., Chen, S., Huang, H., Chen, B., Xiao, X., Lin, J., & Chen, Q. (2015). Novel Anisotropic Janus Composite Particles Based on Urushiol-erbium Chelate Polymer/Polystyrene.

He, W., Song, P., Yu, B., Fang, Z., & Wang, H. (2020). Flame retardant polymeric nanocomposites through the combination of nanomaterials and conventional flame retardants.

Herman, V., Takacs, H., Duclairoir, F., Renault, O., Tortai, J. H., & Viala, B. (2015). Core double–shell cobalt/graphene/polystyrene magnetic nanocomposites synthesized by in situ sonochemical polymerization.

Lock, E. H., & Walton, S. G. (2008). Preparation of Ultra Thin Polystyrene, Polypropylene and Polyethylene Films on Si Substrate Using Spin Coating Technology.

Madani, M., Sharifi-Sanjani, N., Hasan-Kaviar, A., Choghazardi, M., Faridi-Majidi, R., & Hamouda, A. S. (2013). PS/TiO2 (polystyrene/titanium dioxide) composite nanofiber with higher surface to volume ratio prepared by electrospinning: Morphology and thermal properties.

Nitanan, T., Opanasopit, P., Akkaramongkolporn, P., Rojanarata, T., Ngawhirunpat, T., & Supaphol, P. (2011). Effects of processing parameters on morphology of electrospun polystyrene nanofibers.

R., B. (2011). Potential use of fourier transform infrared spectroscopy for identification of molds capable of producing mycotoxins. *Int J Food Prop.*

Ray, S. S., Chen, S.-S., Dan, C. T., Hsu, H.-T., Chang, H.-M., Nguyen, N. C., & Nguyen, H.-T. (2018). Casting of a superhydrophobic membrane composed of polysulfone/Cera flava for improved desalination using a membrane distillation process.

Saltık Çirkin, D., & Yüksek, M. (2021). Fibroin nanofibers production by electrospinning method.

Tanikawa, I., Konuma, M., Hosono, H., & Nakamura, H. (2011). Alternative Plugs Flow Liquid Chromatography (APFLC)/EI-MS System Using a T-shaped Flow Path.

Toy, P. H. (2003). Polystyrene.

Toyran, N. (2008). Fourier Transform Infrared Microspectroscopy Technique: Review. *TURKIYE KLINIKLERI TIP BILIMLERI DERGISI*, s. 704-714.

Tucker, N. S. (2012). The history of the science and technology of electrospinning from 1600 to 1996. Journal of Engineered Fibers and Fabrics.

Volpe, C. D., Siboni, S., Amirfazli, A., Jaroslaw, W. D., & Marmur, A. (2017). Contact angles and wettability: towards common and accurate terminology.

Wu B, H., Saeb A, M. R., Koo B, J. H., & Ramakrishna D, S. (2021). Electrospinning for developing flame retardent polymer materials: Current status and future perspectives.

Xuan, Y. (2010). Preparation of polystyrene spheres in different particle sizes and assembly of the PS colloidal crystals.

Zhao, W., Zhao, H.-B., Cheng, J.-B., Li, W., Zhang, J., & Wang, Y.-Z. (2022). A green, durable and effective flame-retardant coating for expandable polystyrene foams.

APPENDIX

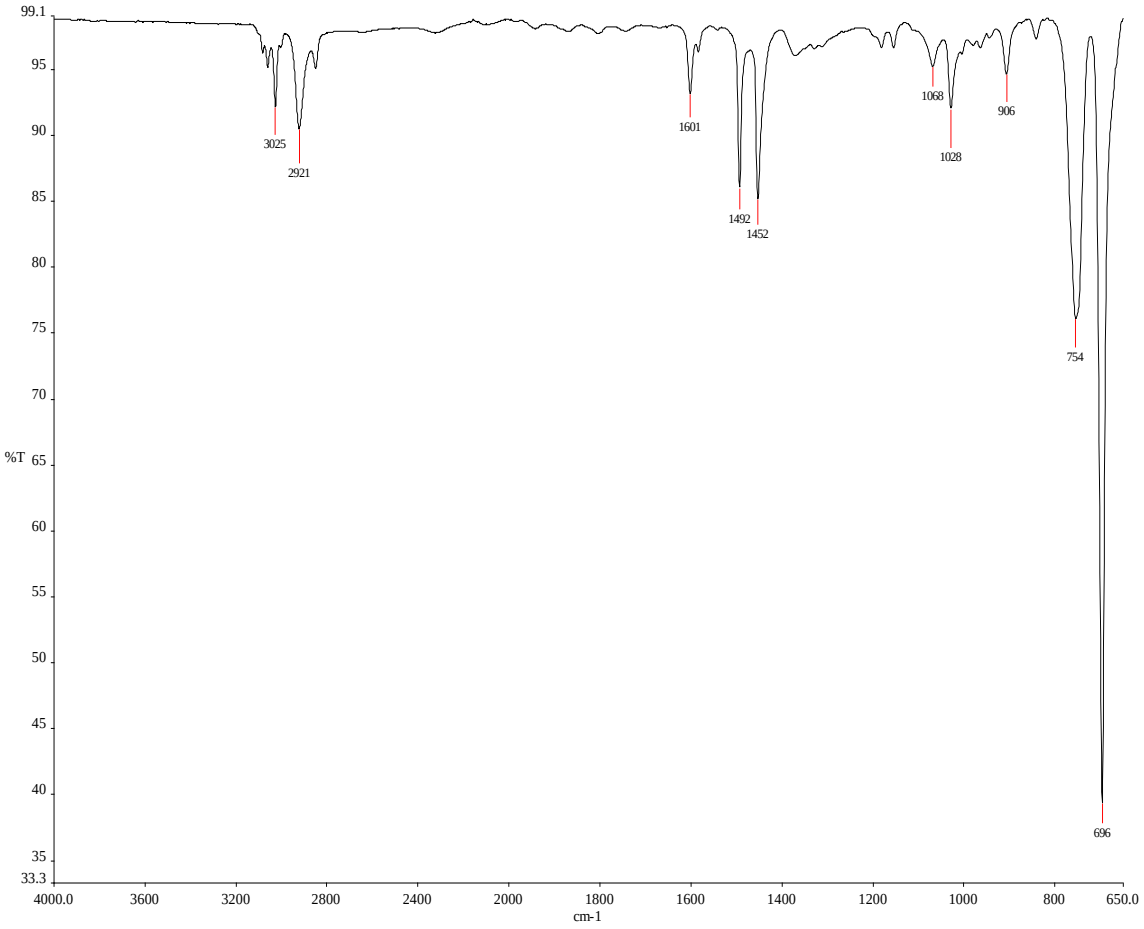
99.1
95
90
85
80
75
70
%T 65
60
55
50
45
40
35
33.3
3025
2921
1601
1492
1452
1068
1028
906
754
696
4000.0
3600
3200
2800
2400
2000
1800
1600
1400
1200
1000
800
650.0
cm-1

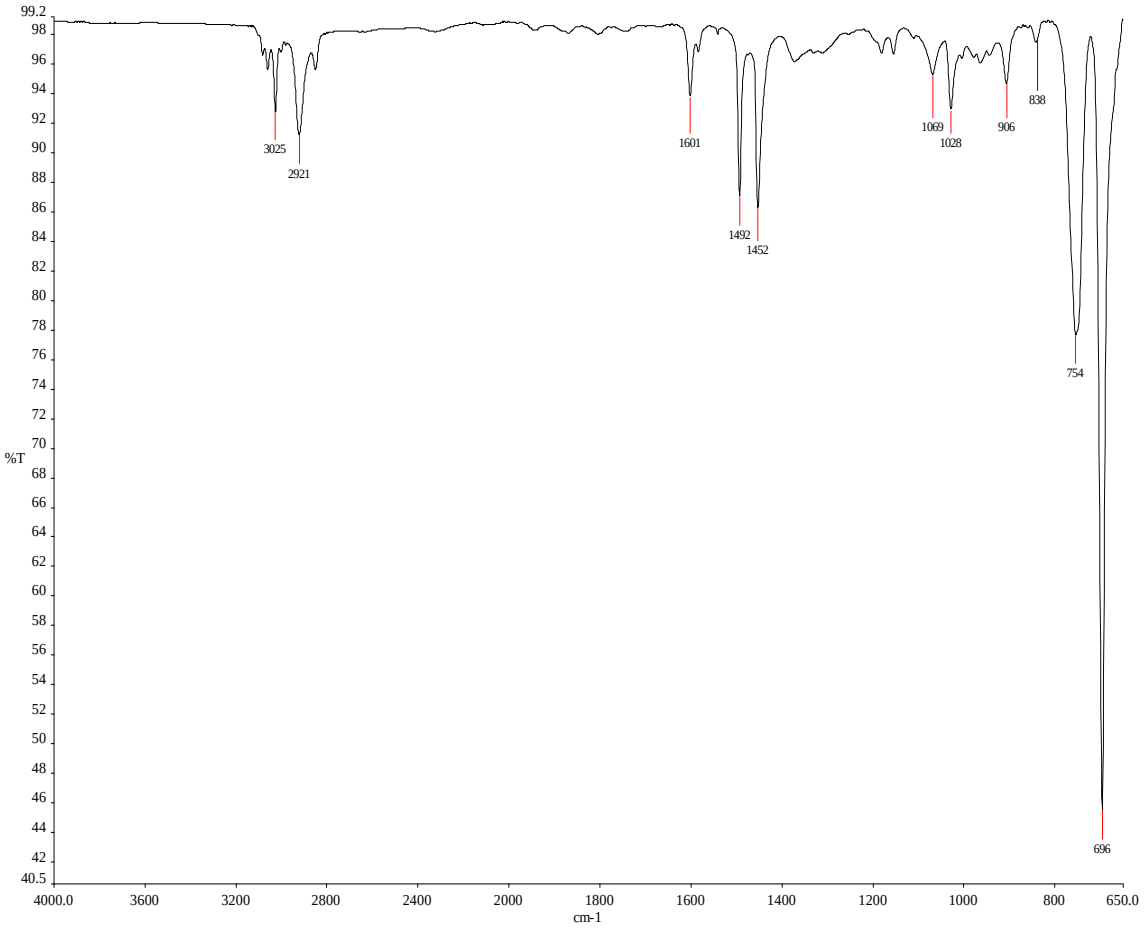
99.2
98
96
94
92
90
88
86
84
82
80
78
76
74
72
70
%T
68
66
64
62
60
58
56
54
52
50
48
46
44
42
40.5
3025
2921
1601
1492
1452
1069
1028
906
838
754
696
4000.0
3600
3200
2800
2400
2000
1800
1600
1400
1200
1000
800
650.0
cm-1

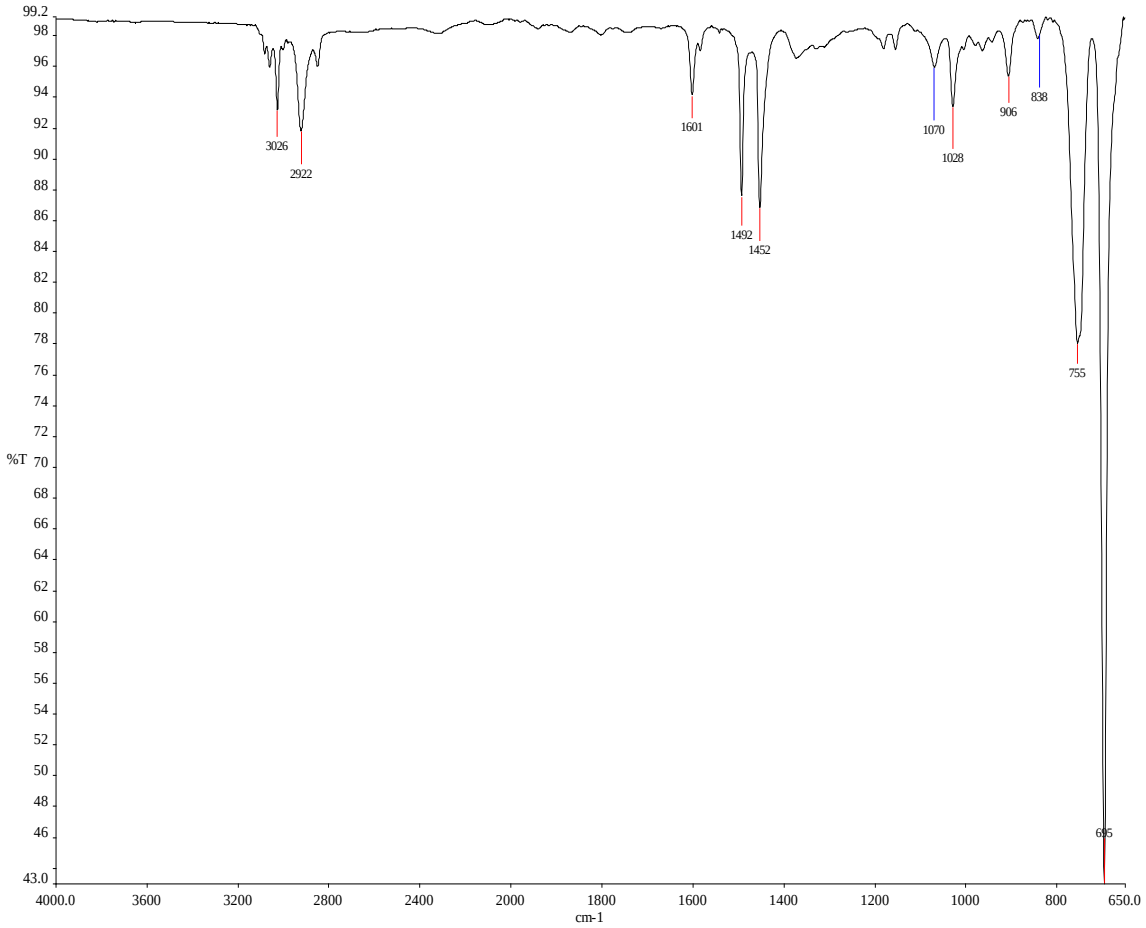
99.2
98
96
94
92
90
88
86
84
82
80
78
76
74
72
%T
70
68
66
64
62
60
58
56
54
52
50
48
46
43.0
3026
2922
1601
1492
1452
1070
1028
906
838
755
695
4000.0
3600
3200
2800
2400
2000
1800
1600
1400
1200
1000
800
650.0
cm-1

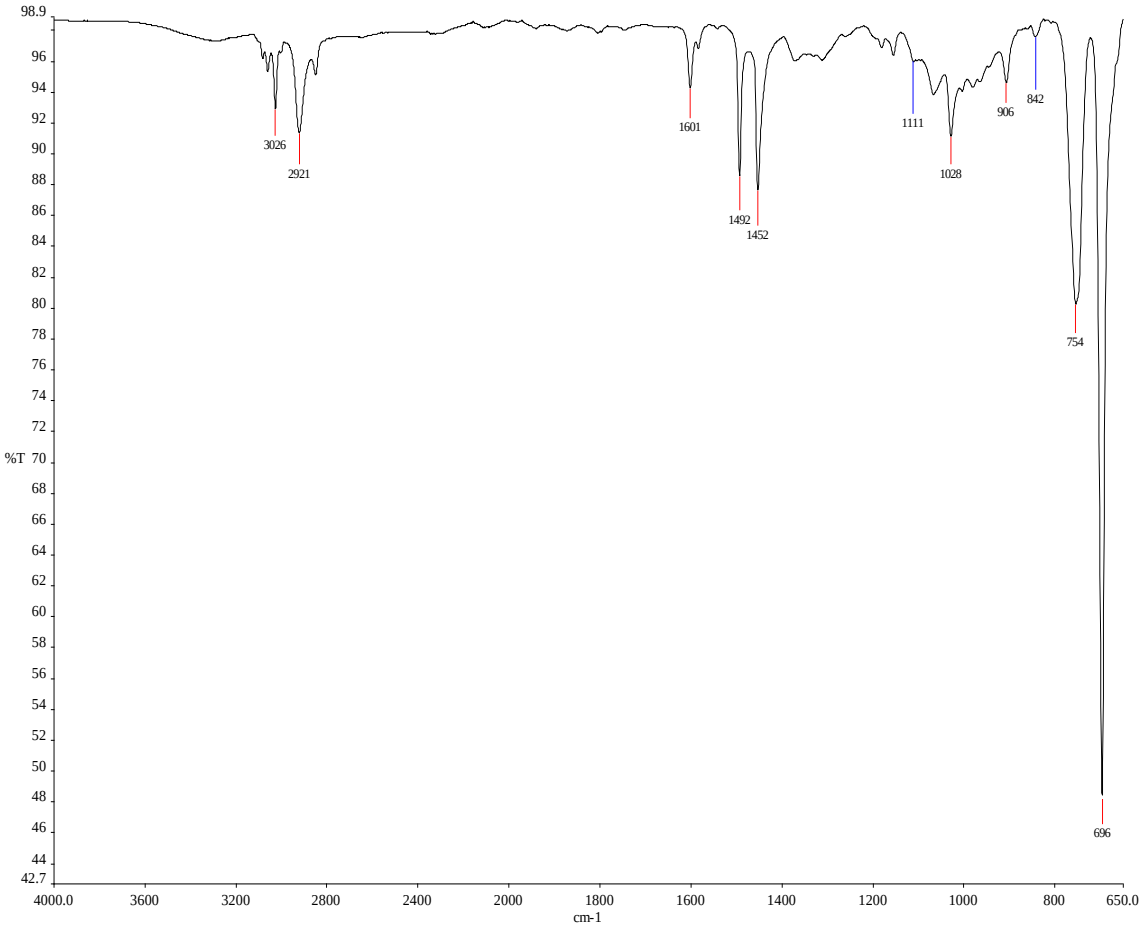
98.9
96
94
92
90
88
86
84
82
80
78
76
74
72
%T 70
68
66
64
62
60
58
56
54
52
50
48
46
44
42.7
3026
2921
1601
1492
1452
1111
1028
906
842
754
696
4000.0
3600
3200
2800
2400
2000
1800
1600
1400
1200
1000
800
650.0
cm-1

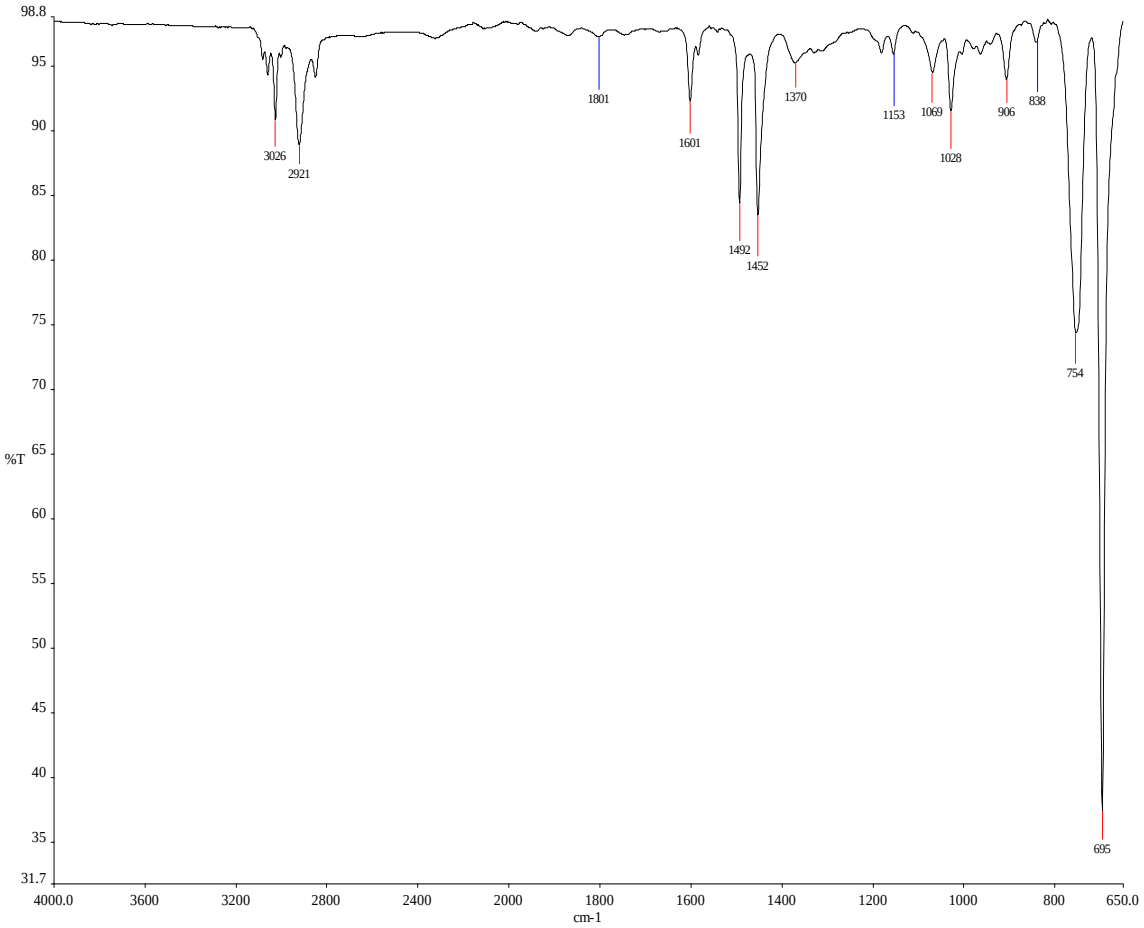
98.8
95
90
85
80
75
70
65
60
55
50
45
40
35
31.7
%T
3026
2921
1801
1601
1492
1452
1370
1153
1069
1028
906
838
754
695
4000.0
3600
3200
2800
2400
2000
1800
1600
1400
1200
1000
800
650.0
cm-1

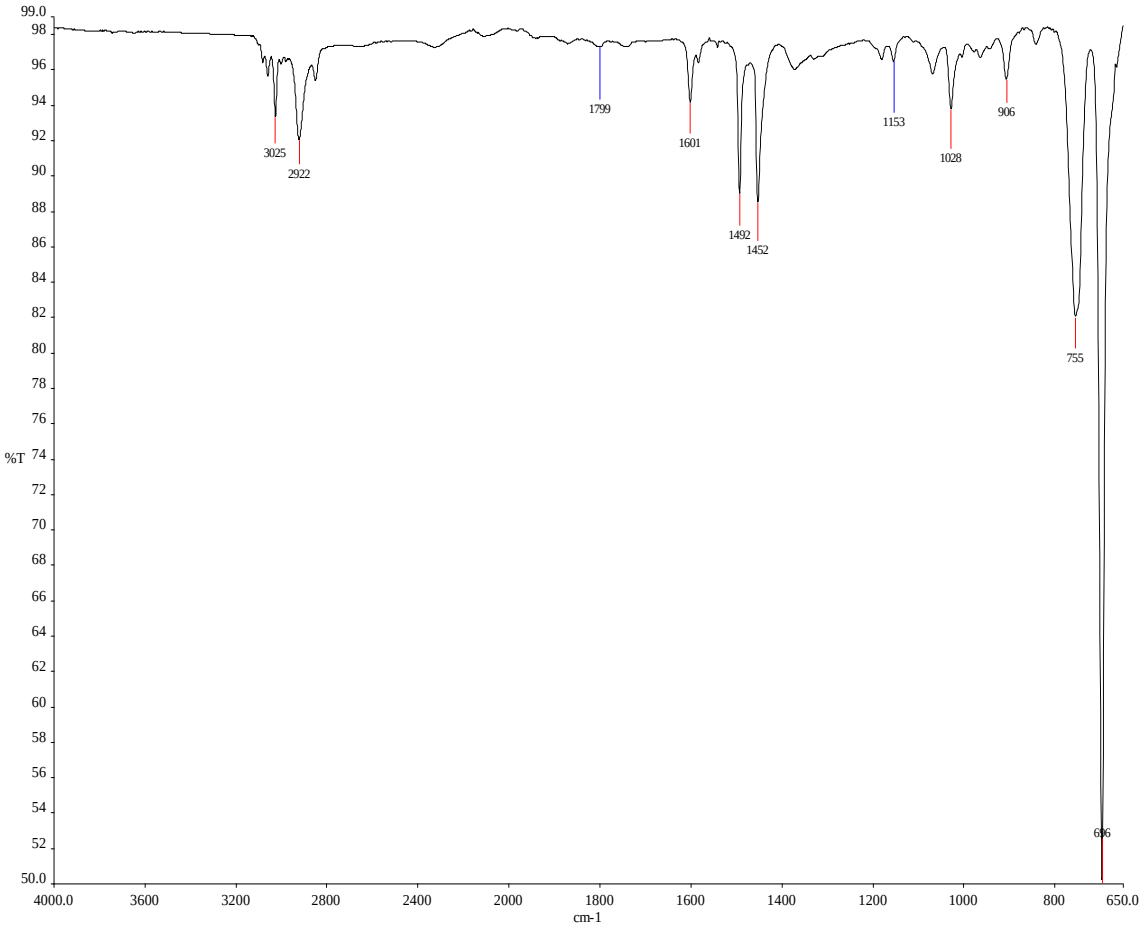
99.0
98
96
94
92
90
88
86
84
82
80
78
76
%T 74
72
70
68
66
64
62
60
58
56
54
52
50.0
4000.0
3600
3200
2800
2400
2000
1800
1600
1400
1200
1000
800
650.0
cm-1
3025
2922
1799
1601
1492
1452
1153
1028
906
755
696